



Numerical validation of compressive strength prediction for hollow concrete blocks

BARBOSA, C.S.¹; HANAI, J.B.²; LOURENÇO, P.B.³

ABSTRACT

The results of a numerical modeling program to evaluate the behavior of hollow concrete blocks under uniaxial compression are addressed. It has been considered appropriate to use interface elements to represent the confinement effect at the top and bottom of blocks. The response of the numerical simulations is compared with experimental data of masonry units. Laboratory tests were carried out utilizing standard flat platens and brush platens to evaluate the confinement effect due block geometry. The elastic and inelastic parameters – compressive strength, tensile strength, stress-strain relationships and fracture energy – were acquired from concrete samples that constitute the blocks. The results from the theoretical analysis are discussed with respect to the ability to reproduce the experimental tests. Good agreement between experimental and numerical results was found for the peak load.

Keywords: *Numerical FEM analysis, laboratory tests, hollow concrete block, non-linear analysis, confinement effect.*

NOTATION

f_c concrete compressive strength;
 f_t concrete tensile strength;
 E elasticity modulus;
 ν Poisson ratio;
 G_f tensile fracture energy;
 G_{fc} fracture energy for compression.

1 INTRODUCTION

The composite behaviour of hollow concrete block masonry still represents a true challenge. The last few years witnessed significant advances in masonry mechanics, both with respect to experimental testing and to numerical modelling. A particular case is hollow concrete block masonry in which the units are structures constituted by slender walls, interacting between themselves and usually featuring different geometries. The mechanical properties of the concrete from the blocks are usually not known, since tests are carried out on full blocks.

With respect to the difficulty of characterizing the materials that constitute masonry in laboratory tests, it should be emphasized that tests carried out on masonry units with flat platens provide an artificial compressive strength due the restraint effect, that the post-peak behaviour in compression is

¹ Assistant Professor, University of Campinas, Department of Structural Engineering, Brazil, claudiusbarbosa@yahoo.com.br

² Professor, University of Sao Paulo, Department of Structural Engineering, Sao Carlos, Brazil. jbhantai@sc.usp.br

³ Professor, ISISE, University of Minho, Department of Civil Engineering, Guimaraes, Portugal. pbl@civil.uminho.pt

usually not determined, that the fracture energy in compression (G_{fc}) depends significantly on the test set-up and equipment, that the load conditions of units and mortar tests do not reproduce the state of stress of the composite inside the masonry and that the mortar specimens cast in steel moulds do not represent real curing conditions (Stöckl et al. 1994 [1]).

In order to carry out sophisticated numerical analyses, it is necessary to further advance in the characterization of the properties of masonry materials and assemblies (Marzahn 2003 [2]; Pina-Henriques and Lourenço 2006 [3]). One example of an attempt to provide detailed information on the behavior of hollow block masonry has been made by modeling behavior of a prism formed using a block whose Young's modulus was obtained from tests on samples extracted from concrete blocks (Hamid and Chukwunyenye 1984 [4]). Similarly, tests have been performed on samples extracted from hollow concrete, calcium silicate and solid concrete blocks to identify the compressive and tensile strength, together with the Young's modulus (Hawk et al. 1997 [4]; Ganzerli et al. 2003 [6]; Marzahn 2003 [2]).

Considerable difficulties are therefore expected in any research aiming at characterizing the mechanical properties of masonry components. For this reason, the present paper adopts a different approach to ensure adequate definition of the stress-strain relationship of masonry components. Laboratory tests were carried out on hollow concrete blocks and concrete samples that constitute the masonry units. The adopted technique was to mold the blocks in the laboratory using a concrete mix also used to cast concrete samples (Barbosa, Lourenco and Hanai 2009 [7]).

Modeling of masonry itself is a complex task due to the heterogeneity and orthotropy caused by masonry components and their interfaces. Mortar joints, for example, act usually as planes of weakness and, depending of the level of accuracy and the simplicity, micro-modeling of individual components, block and mortar, or macro-modeling of masonry as a composite can be adopted (Lourenço 1996 [8]). In the case of masonry compression failure, discontinuum models showed clear advantages when compared to continuum models, based on plasticity and cracking, in predicting the compressive strength and peak strain of solid brick prisms from the properties of the constituents (Pina-Henriques and Lourenço 2006 [3]; Lourenco and Pina-Henriques 2006 [8]). This is true for solid masonry, whereas for hollow block masonry the application of such models seems cumbersome due to the geometrical complexity of the basic masonry cell. With hollow blocks, their slenderness introduces another difficulty to be represented in numerical models under compression.

In addition, the flat steel plate above the block in the test set-up provides a uniform stress-strain distribution during the test. Platen restraint induces a complex triaxial stress state at the ends of blocks and, consequently, an increase of the compressive strength. It is also possible to bend the steel plate if it is not stiff (Barbosa and Hanai 2008 [11]).

If the test is carried out with high stiffness plates, the unit ends have the same lateral strain as the platen and shear stresses are developed between them inducing a triaxial stress state in that region. The opposite condition – low stiffness and high Poisson ratio –, means “apparent” shear stresses are developed in interfaces with cracks arising (Ferro 2006 [12]). Figure 1 represents this phenomenon.

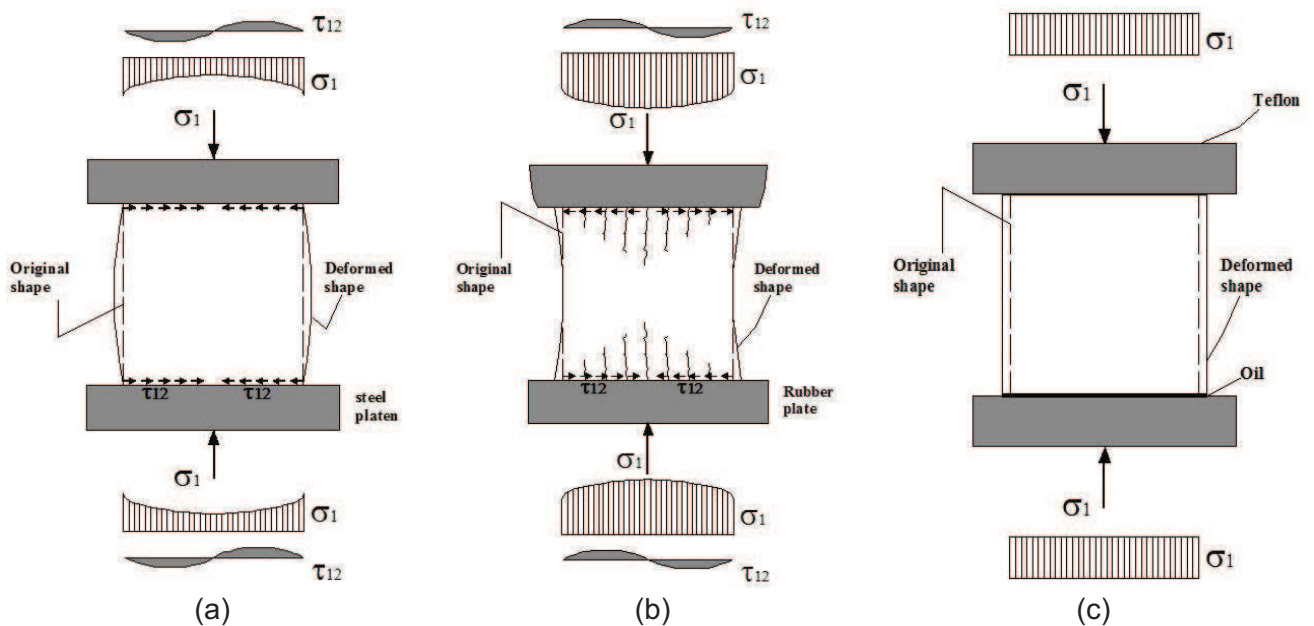


Figure 1. Loading platen influence: stiff steel plate (a); rubber plate (b); steel plate and teflon (c).

In this research program, the numerical analysis is based on continuum finite elements utilizing a commercial non-linear finite element code DIANA (DIANA 2005 [10]). Four different concrete strengths were simulated, utilizing the parameters obtained from the experimental program to validate the constitutive behavior obtained in masonry units. To represent the confinement effect induced for steel plates, it was considered appropriate to use interface elements and restrained nodes. Laboratory tests were carried out utilizing standard flat platens and brush platens to evaluate the confinement effect due block geometry. It is shown that good agreement between experimental and numerical result can be obtained in the prediction of the peak load of blocks using advanced numerical simulations.

2 BRIEF OF TEST METHOD

Both hollow concrete blocks and concrete cylindrical samples were moulded with plastic consistency. The same moulding procedures were adopted in casting, vibrating, curing and finishing. The blocks and samples were molded in four concrete strengths (13 N/mm², 22 N/mm², 26 N/mm² and 30 N/mm²) related to axial compression test with cylindrical samples 100 x 200 mm high.

Steel moulds were utilized to prepare concrete blocks. Internal cores were provided by two EPS (Expanded Polystyrene) blocks fixed to the steel mould. The blocks were manufactured in laboratory to assure the desired concrete strength, high quality control and precise geometry. Hollow concrete blocks, 140 x 190 x 390 mm external dimensions and 30663 mm² net area, as shown in Figure 2a were produced.

Simultaneously, cylindrical samples (100 x 200 mm) were also produced with the same material. Both elements were submitted to axial compression and split tensile tests. The block compression tests were performed with flat steel platens and brush platens in a servo-hydraulic machine and tested in the linearly controlled displacement mode. The controlled displacement mode allows the acquisition of the stress-strain diagram, including its descending or softening branch.

The top and bottom of blocks and samples were smoothed in an appropriate abrasion machine as can be seen in Figure 2b.

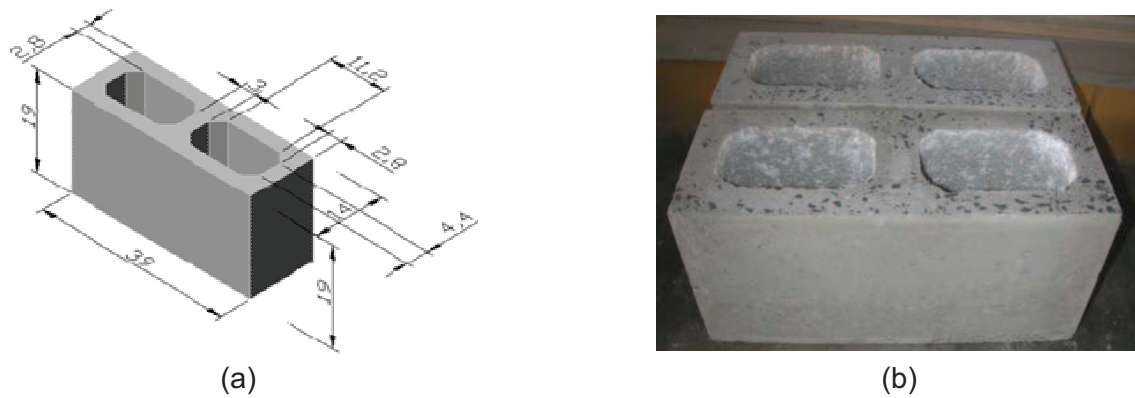


Figure 2. a) Block geometry (a), in centimeters, and flat top or bottom (b).

The distribution of the applied force was achieved with a 35 mm thick rectangular steel platen (200 x 400 mm). On the top of the block, the contact of this platen with the loading system was done with a 294 mm diameter rigid steel cylinder. On the base, there was a very rigid and large steel block.

Five displacement transducers (base length = 100 mm) were positioned on the blocks along vertical reference lines to measure the average strain. In addition, two displacement transducers were positioned to obtain the horizontal strains at the top of the block. The strain measurement in the concrete samples was taken with two displacement transducers. Figure 3 illustrates the location of transducers in blocks. The numbers indicate the point of vertical displacement measurement and the letters the transvers ones. In the standard block compression tests there were four displacement transducers used to measure the whole set of platen displacement readings.

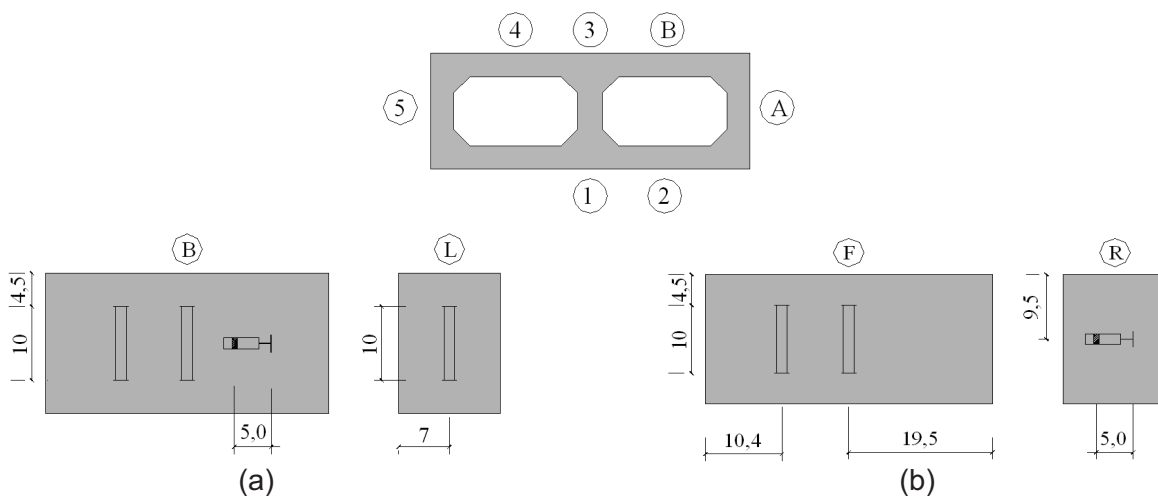


Figure 3. Instruments located throughout face-shell and webs (centimeters).

Figure 4 illustrates the block test with the standard platen and brush platen. Transversal stresses occur in the tested element due the friction between steel platen and the unit top and bottom. Transversal stresses prevent the free deformation of the top and bottom regions and its magnitude depends directly on the geometric shape of the element. Measured compressive strength increases to a value that does not correspond to a perfect axial compression test. The brush platen test can provide a better evaluation of mechanical properties of the block since it reduces the confinement effect. The slender steel sticks transfer the applied forces and they allow almost free transversal displacements at the top and the bottom of the blocks. The steel sticks have a cross section of 5.1 mm diameter and are 110 mm in length; this relationship ensures a significant reduction of lateral restraint.

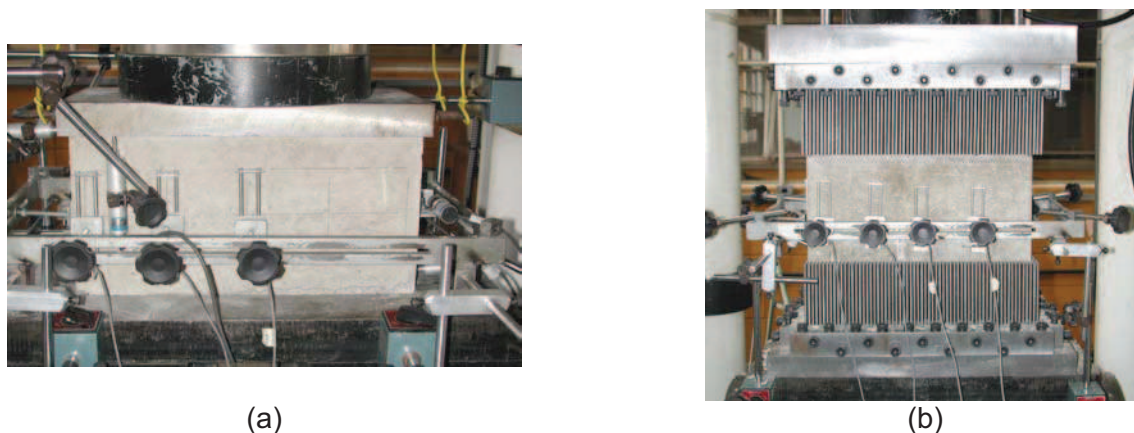


Figure 4. Block compression tests: flat steel platen (a) and brush platen (b).

To evaluate the tensile strength of concrete samples, tensile splitting tests were done with displacement control. In addition 150 x 150 x 500 mm concrete beams were molded and three-point bending test were carried out to evaluate the tensile flexural strength and fracture energy.

In standard compression tests, inclined cracks arose typically at about 80% of the ultimate load along the larger face of the blocks. These cracks were of crushing type and they were succeeded by progressive spalling. Internally to the block, the critical cracks proceeded along an inclined plane, towards the transversal webs. The failure mode occurred due to the particular block geometry and its ratio of width and height, resulting in a significant confinement effect derived from the platen action.

In the modified compression tests, the cracks arose starting from 50% of the maximum load in the face-shells. They were vertical cracks up to the peak force. In the web regions, vertical cracks were noted near the peak force. Post-peak cracks spread throughout the face-shells and webs and several inclined cracks showed up like in standard tests.

3 NUMERICAL MODELING

The numerical simulations were carried out with continuum finite elements utilizing a micromodeling strategy, in which mortar and concrete are represented individually with non-linear behaviour. An incremental-iterative Newton-Raphson method with arc-length control and line-search technique was adopted to solve the resulting non-linear equilibrium equations (DIANA 2005 [10]). The load steps were adjusted manually, reducing the step size whenever divergence of the iterative process was found.

Previous analyses with hollow concrete block prisms showed that the plane strain and plane stress approach is not accurate, in comparison to three-dimensional analyses, and the behaviour obtained in tests (Barbosa, Lourenço and Hanai 2006 [7]). 3D analysis remains computationally very demanding and the use of simplified two-dimensional approaches is of relevance for the application of a numerical toolbox for strength prediction of hollow concrete masonry. This research nevertheless is based on 3D-analysis. Drucker-Prager was combined with smeared cracking with a straight tension cut-off, exponential tension softening and variable shear retention.

Figure 5a depicts the basic cell defined to represent the block – a quarter full height –, and the mesh adopted for the numerical simulations Figure 5b. The boundary conditions assume symmetry. The load was applied as a set of uniformly distributed displacements at the top of the quarter cell. All the nodes at the top and bottom of the model were restrained in three directions (x, y and z axis) to simulate the friction test condition.

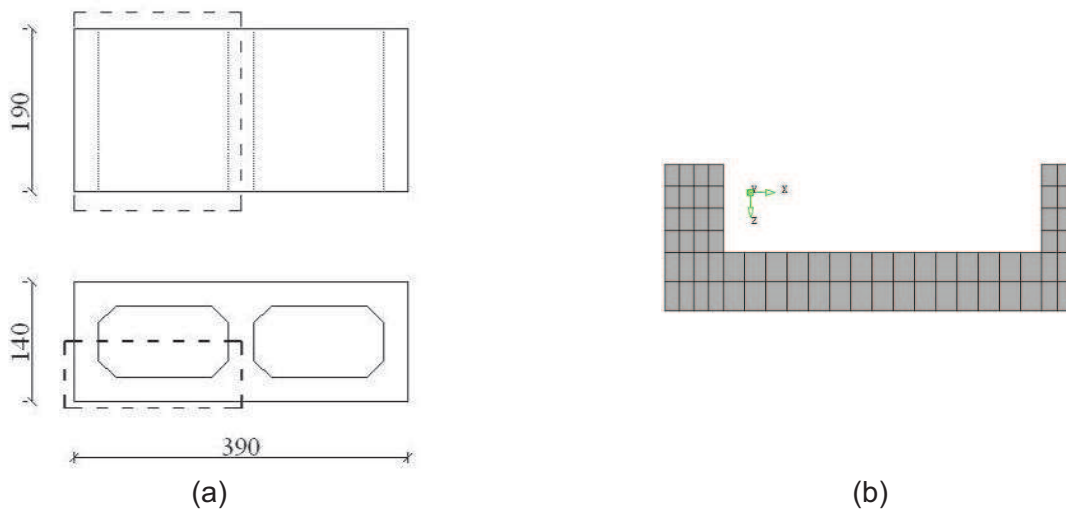


Figure 5. Basic cell of hollow concrete block: a quarter of full height hollow block (a); element finite mesh top view (b) – dimensions in millimeters.

It is important to highlight that the cracks, the boundary effects of the model and the failure modes are not symmetric in the tests, even if it is noted that these phenomena induce changes mainly in the post-peak behavior.

The three-dimensional mesh includes 1320 twenty-noded brick CHX60 elements (7441 nodes), with a quadratic interpolation and 3x3x3 Gauss integration. A more accurate model considered the reduction of confinement effect by means of plane interface elements discretization between steel plate and block top and bottom (1716 CQ48I elements and 9399 nodes). The Interface element has no thickness.

A friction angle $\phi = 10^\circ$ and dilatancy angle $\psi = 5^\circ$ was adopted. With the exception of these values, all other values requested by the constitutive models have been outlined in detail in the previous section, having been obtained directly via experimental testing.

From the cylindrical test the elastic and inelastic parameters presented in Table 1 were defined for the four concrete strength groups. Here, f_c is the compressive strength, f_t is the tensile strength, E is the elasticity modulus, ν is the Poisson ratio (with approximated values) and G_f is the tensile fracture energy.

Table 1. Elastic and inelastic properties of concrete.

Block	f_c	f_t	E	ν	G_f
	(N/mm ²)			-	(N/mm)
B1	13,4	1,5	18080	0,20	0,093
B2	22,1	2,3	24476	0,20	0,107
B3	26,0	2,6	23956	0,20	0,122
B4	30,9	2,8	23004	0,20	0,154

In Table 2 the three models of confinement are analyzed and the linear mechanical properties of the interface are noted. k_v represents vertical stiffness and k_t the transversal stiffness. These

parameters were defined randomly, based on the block behaviour model. Model C is an attempt to represent the brush platen test.

Table 2. Confinement model and linear stiffness of interface.

Confinement model	k_v (N/mm ³)	k_t (N/mm ³)
A (full confinement)	Restrained nodes	
B (intermediate confinement)	2,89	11,91
C (no confinement)	0,61	0,11

4 COMPARISON OF EXPERIMENTAL AND NUMERICAL RESULTS

The numerical and experimental results are compared by peak load and stress-strain diagram. Table 3 summarizes peak loads obtained in theoretical and experimental models. The differences between them are around 9%.

Table 3. Comparison between the numerical and experimental ultimate force and strain.

Block	F^{exp} (modified test)	F^{exp} (standard test)	F^{num}	$\frac{F^{\text{num}}}{F^{\text{exp}}}$	$\varepsilon_u^{\text{exp}}$	$\varepsilon_u^{\text{num}}$	$\frac{\varepsilon^{\text{num}}}{\varepsilon^{\text{exp}}}$
	(kN)				(μ)		
B1	319	389	399	1,03	883	1199	1,36
B2	597	813	650	0,80	1464	1580	1,08
B3	696	871	822	0,94	1727	1705	0,99
B4	727	935	1003	1,07	1437	1892	1,32

The stress-strain diagrams are depicted in Figure 6. Note for each group there are represented three lines two referring to experimental results and one to the numerical model. For all groups (B1 to B4) the numerical model presents lower stiffness than experimental results and with B1 ultimate strain is 36% higher for the numerical model. Boundary conditions of finite element models cause these differences. While the nodal restraint are represented as no displacement in all top and bottom nodes, this performance during the test is only approximated. It is necessary to evaluate better the behaviour of block-platen interface to implement an accurate condition for numerical models.

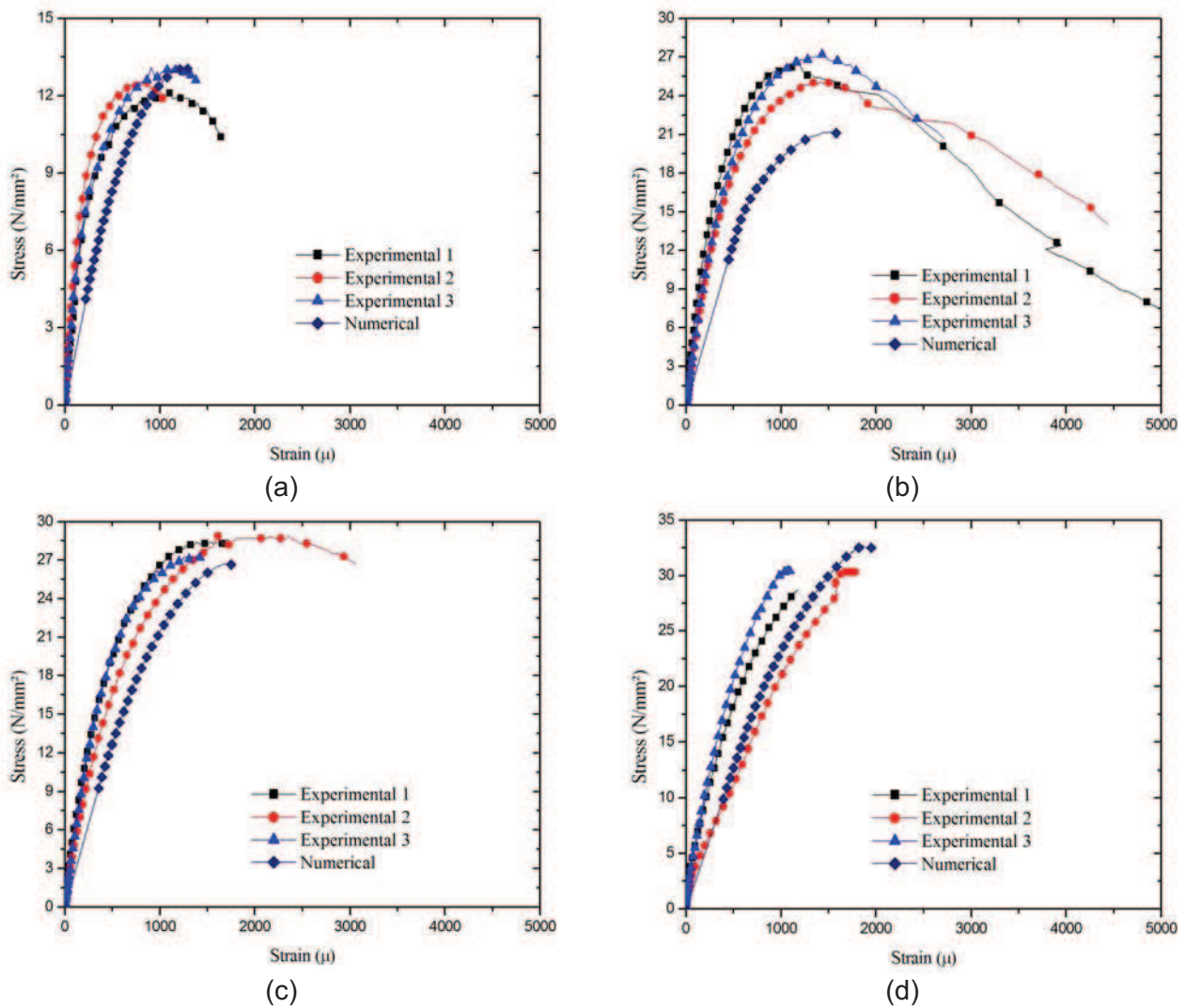


Figure 6. Stress-strain experimental and numerical diagrams: B1 (a); B2 (b); B3 (c) e B4 (d).

Figure 7 presents stress-strain relationships for the confinement models presented in Table 2. The peak loads obtained in model C (no confinement) and B (intermediate confinement) present 1% divergence. Model A (full confinement) present peak loads 6% higher than the others based on the adopted stiffness parameters. This analysis refers to group B3. The differences between standard and modified tests are close to 20% but the numerical model provides differences close to 6%. Therefore, numerical Model C shows some modifications when compared to model A but more accurate studies must be developed for interface behaviour. The knowledge of stress and strain distribution throughout face shells can identify the next analysis steps.

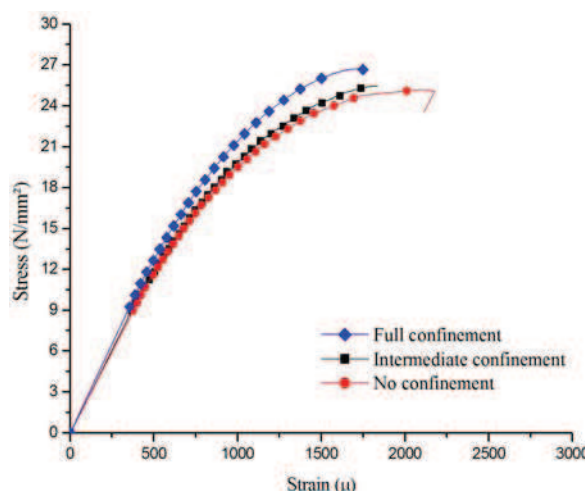


Figure 7. Stress-strain numerical diagrams considering distinct boundary conditions.

5 CONCLUSION

Numerical model considering Drucker-Prager combined with smeared cracking with a straight tension cut-off, exponential tension softening and variable shear retention represents with good accuracy the hollow concrete blocks behaviour under compression.

Most of the parameters for the numerical models were obtained from a concrete sample test program using material manufactured with the same zero slump concrete as hollow blocks. The adopted procedure ensures identical mechanical properties for the blocks and the samples that guarantees accurate comparison of results.

The peak load of numerical undertaken was close to the test values. The same occurred in the comparison of stress-strain relationships.

The numerical model considering interface elements does not represent with satisfactorily the brush-platen test. More accurate conclusions will be reached after stress, strain analysis across faces shells and webs is undertaken and considers the distinct confinement levels.

ACKNOWLEDGEMENTS

The authors would like to acknowledge FAPESP – Sao Paulo State Research Support Foundation – and CAPES – Brazilian Research Support Foundation – for the financial support given to this research.

REFERENCES

- [1] Stöckl, S., Bierwirth, H., and Kupfer, H. The influence of test method on the results of compression tests on mortar. In: *International Brick and Block Masonry Conference*, 10, Calgary, Alberta, Canada.1994.
- [2] Marzahn, G.A. Extended investigation of mechanical properties of masonry units. In: *North American Masonry Conference*, 9., Clemson, South Carolina, USA, 813-824. 2003.
- [3] Pina-Henriques, J.L., Lourenço, P.B. *Masonry compression: a numerical investigation at the meso-level*. Engineering Computations, 23(4), 382-407. 2006.
- [4] Hamid, A.A.; Chukwunye, A.O. *Compression behavior of concrete masonry prisms*. Journal of Structural Engineering, 112(3), 605-13. 1986.
- [5] Hawk, S.W., McLean, D.I.; Young, T.C. *Compressive behavior of insulated concrete masonry prisms*. The Masonry Society Journal, 15(2), 53-60. 1997.

- [6] Ganzerli, S. et al. Compression strength testing for nonstandard concrete masonry units. *North American Masonry Conference*, 9., Clemson, South Carolina, USA, 60-71. 2003.
- [7] Barbosa, C.S; Lourenço, P.B.; Hanai, J.B. *On the compressive strength prediction for concrete masonry prisms. Materials and Structures*, v. DOI 10, p. DOI 10.1617/s11, 2009.
- [8] Lourenço, P.B. *Computational strategies for masonry structures*. Delft University Press: The Netherlands. 210p. Available from < www.civil.uminho.pt/masonry>. 1996.
- [9] Lourenço, P.B., Pina-Henriques, J.L. *Masonry micro-modelling: a continuum approach in compression*. *Computers & Structures*, 84(29-30), 1977-1989. 2006.
- [10] DIANA. *Finite Element Code: User's Manual – Release 9*. TNO Building and Construction Research: Delft, The Netherlands. 2005.
- [11] Barbosa, C.S.; Hanai, J.B. Deformability of hollow concrete blocks and platen effect on axial compression tests. In: *International Brick & Block Masonry Conference*, 14, 2008, Sydney, Australia. 2008.
- [12] Ferro, G. *On dissipated energy density in compression for concrete*. *Engineering Fracture Mechanics*, v.73, pp. 1510-30. 2006.